The Impact of Transmission Power Control Strategies on Lifetime of Wireless Sensor Networks

Huseyin Cotuk, Kemal Bicakci, Bulent Tavli, and Erkam Uzun

Abstract—Transmission power control has paramount importance in the design of energy-efficient wireless sensor networks (WSNs). In this paper, we systematically explore the effects of various transmission power control strategies on WSN lifetime with an emphasis on discretization of power levels and strategies for transmission power assignment. We investigate the effects of the granularity of power levels on energy dissipation characteristics through a linear programming framework by modifying a well known and heavily utilized continuous transmission power model (*HCB* model). We also investigate various transmission power assignment strategies by using two sets of experimental data on Mica motes. A novel family of mathematical programming models are developed to analyze the performance of these strategies. Bandwidth requirements of the proposed transmission power assignment strategies are also investigated. Numerical analysis of our models are performed to characterize the effects of various design parameters and to compare the relative performance of transmission power assignment strategies. Our results show that the granularity of discrete energy consumption has a profound impact on WSN lifetime, furthermore, more fine-grained control of transmission power (i.e., link level control) can extend network lifetime up to 20% in comparison to optimally-assigned network-level single transmission power.

Index Terms—Wireless sensor networks, discrete power levels, mathematical programming, linear programming, mixed integer programming, energy efficiency, bandwidth, network lifetime, transmission power control

1 Introduction

Prolonging network lifetime is one of the most important design goals for Wireless Sensor Networks (WSNs) [1], [2]. Since in general WSN energy expenditure is heavily dominated by communication energy [3], there is a vast literature on strategies (e.g., optimal routing [4], data aggregation [5], and many others [3]) for optimizing the converge-cast traffic, which is the typical communication pattern in WSN applications. In many studies on energy efficiency of WSNs, the assumption of a capability for performing power adjustments on a continuous range is made (i.e., each sensor node can fine-tune its transmission energy adaptively and dissipate the exact amount of energy to reach the intended recipient) [6]-[9]. However, it is known that in practical settings power level assignment is limited to a discrete set of values. In some cases, it is not even viable or preferable to adapt the transmission power dynamically [10], [11], hence, transmission power control in some practical cases reduces to pre-setting all nodes with a single level before the deployment and not changing the settings throughout the whole network lifetime.

Transmission power control in WSNs has already been studied extensively in the literature [12]. All transmission power assignment strategies studied so far can be classified into one of the three major categories: network-wide, node level, and link level solutions [13]. While it is evident that more fine-tuned power assignment does not waste energy and, thus, increases lifetime, the net impact of various transmission power assignment strategies on network lifetime remains unclear. Our work presents a framework which enables us to quantify the impact and to make a systematic comparison of various strategies. More precisely stated, in this paper our objective is to seek answers to the following research problems:

1) With the provided level of transmission power granularity, how much degradation with respect to network lifetime should be expected as compared to the case of continuous power in which transmission power can be adjusted in perfect granularity? How do positioning errors and packet reception rates affect these results?
2) Is it necessary to utilize all available transmission power levels to optimize the network lifetime? Can we maximize the network lifetime by employing a selected subset of available transmission power levels?
3) Can we improve the network lifetime significantly by assigning a potentially different power level for each link (i.e., transmission power levels assigned for different outgoing links of a node are allowed to be in different levels) instead of assigning a single level to each node (i.e., all outgoing flows of each node use the same transmission power)?
4) What is the impact of assigning a single transmission power level to all nodes in the network globally instead of choosing optimal power level for each individual sensor node on the network lifetime?
5) In applications where a single global transmission power level should be set and used throughout the

• *The authors are with TOBB University of Economics and Technology, Ankara, Turkey. E-mail: {hcotuk, bicakci, btavli, euzun}@etu.edu.tr.*

Manuscript received 14 Sep. 2012; revised 12 July 2013; accepted 20 July 2013. Date of publication 30 July 2013; date of current version 14 Oct. 2014. Recommended for acceptance by K. Roemer.
For information on obtaining reprints of this article, please send e-mail to: reprints@ieee.org, and reference the Digital Object Identifier below.
Digital Object Identifier no. 10.1109/TC.2013.151

0018-9340 © 2013 IEEE. Personal use is permitted, but republication/redistribution requires IEEE permission.
See http://www.ieee.org/publications_standards/publications/rights/index.html for more information.

$$E_{rx} = E_{rx}^{C-HCB} = \rho \quad (1)$$

$$E_{tx}(d_{ij}) = E_{tx}^{C-HCB}(d_{ij}) = \rho + \varepsilon d_{ij}^{\alpha} \quad (2)$$

Fig. 1. Continuous *HCB* energy model.

$$E_{rx} = E_{rx}^{D-HCB} = \rho \quad (3)$$

$$E_{tx}(d_{ij}) = E_{tx}^{D-HCB}(d_{ij}) = \rho + \eta \left\lceil \frac{\varepsilon d_{ij}^{\alpha}}{\eta} \right\rceil \quad (4)$$

Fig. 2. Discrete *HCB* energy model.

whole network lifetime, is there a simple, yet, effective strategy for choosing the power level?

6) What are the bandwidth requirements of power level assignment strategies? In other words, what is the effect of source data rate on network lifetime for different power level assignment strategies?

Our methodology is to investigate the aforementioned open research problems by using a novel family of Mathematical Programming (MP) models. Choosing an MP based analysis method has a number of advantages. One of them is the abstraction from implementation details which enables us to analyze the impact of discrete power level models from an energy efficiency perspective within a general framework and without considering any specific protocol or algorithm. This approach abstracts us away from the overhead or shadowing effects brought by a specific protocol. Since proposing a protocol or an algorithm is not our goal, the analysis presented in this paper does not compete with earlier such efforts. On the other hand, a comprehensive characterization of the impact of power level assignment strategies on network lifetime in WSNs is a novel research contribution and may provide valuable insights for the design of future protocols.

As examples of MP models, both Linear Programming (LP) and Mixed Integer Programming (MIP) are used to find the best solution considering a given set of constraints, which characterize the set of legitimate decisions. Alternative decisions are compared based on their objective function values and the one with the best value (can be the smallest or the largest depending on the nature of the function) is selected as the optimal. Although they are used for the same reason, LP and MIP models cannot be used in place of each other in many occasions. Basically, the types of decisions to be made determine which type of a mathematical model should be used to model the problem under consideration [14], which leads to both LP and MIP models for the research problems we investigate.

The rest of the paper is organized as follows. Section 2 explores the impact of power level granularity on the achievable network lifetime by revisiting the HCB energy model. We investigate the effects of transmission power control imperfections in the HCB energy model on network lifetime due to positioning errors in Section 3. In Section 4, we modify the HCB energy model to account for packet errors and the probabilistic nature of path loss and characterize the effects of this model on network lifetime. In Section 5 and Section 6, we build a family of MP models by taking a more practical point of view using two data sets validated by real hardware measurements. In Section 7, numerical analysis by using the MP models developed in two preceding sections are performed. Section 8 explores the relationship between power control strategies and bandwidth requirements in the context of network lifetime maximization problem. Section 9 reviews the related work and compares our results with earlier studies. Section 10 provides our concluding remarks.

2 Revisiting *HCB* Energy Model

The seminal work by Heinzelman, Chandrakasan, and Balakrishnan [15] introduces a useful model for radio hardware energy dissipation of wireless sensor nodes. Many later studies adopt exactly the same (e.g., [3]) or very similar models (e.g., [4]). Due to its widespread use, we first revisit the Heinzelman-Chandrakasan-Balakrishnan (*HCB*) energy model presented in Fig. 1.

In the original what we call "continuous" *HCB* model, E_{rx}^{C-HCB} and E_{tx}^{C-HCB} refers to the amount of energy to receive and transmit a bit, respectively. The constant ρ (50 nJ) denotes the energy dissipation on electronic circuitry, ε (100 pJ) shows the transmitter efficiency and α (2 for free space model) denotes the path loss.

As we have noted earlier, one of the limitations of continuous *HCB* energy model is the assumption of the adjustability of the transmission energy in a continuum. To investigate the effects of discrete transmission power levels, we introduce a modification to this model and propose the "discrete" *HCB* model as presented in Fig. 2.

In this model, the amount of energy to transmit and receive a bit is represented by E_{tx}^{D-HCB} and E_{rx}^{D-HCB}, respectively. Here, electronics energy remains unchanged but transmitter's energy can be adjusted only using discrete levels, which are integer multiples of minimum energy quantum (η). Notation $\lceil\ \rceil$ is used to denote the ceiling function, which rounds the argument to the closest integer larger than or equal to the argument (e.g., $\lceil 4.01 \rceil = 5$).

In our system model, energy consumption of sensor nodes is dominated by communication energy dissipation rather than sensing and processing energy dissipations (energy factors such as sleep-mode energy are also ignored for the sake of simplicity). This assumption is supported by the results of experiments in actual WSN testbeds [16]. In our framework, we assume that there is a single base station and N sensor nodes. Time is organized into rounds with duration T_{rnd}. Each sensor node-i creates the same amount of traffic (s_i) at each round to be conveyed to the base station (i.e., sensor nodes create constant bit rate-CBR-flows). Traffic generated at each node terminates at the base station either by direct transfer or through other sensors acting as relays. The network topology is represented by a directed graph $G = (V, A)$. V is the set of all nodes, including the base station as node-1. We also define set W, which includes all the nodes except the base station (i.e., $W = V \backslash \{1\}$). $A = \{(i, j) : i \in W, j \in V - i\}$ is the set of arcs (links). Note that the definition of A implies that no node sends traffic to itself and the base station does not send out any traffic to the sensor nodes. The amount of traffic that flows from node-i to node-j is represented as f_{ij}.

We assume that a TDMA-based MAC layer is in operation and a time-slot assignment algorithm outputs a conflict-free transmission schedule. In [17], it is shown that such an algorithm is possible, hence, collision free communication is achieved if bandwidth requirements are satisfied. We defer

Maximize t
Subject to:

$$f_{ij} \geq 0 \ \forall (i,j) \in A \quad (5)$$

$$\sum_{j \in V} f_{ij} = s_i t + \sum_{j \in W} f_{ji} \ \forall i \in W \quad (6)$$

$$f_{ij} = 0, \text{if } d_{ij} \geq R_{max} \ \forall (i,j) \in A \quad (7)$$

$$E_{rx} \sum_{j \in W} f_{ji} + \sum_{j \in V} f_{ij} E_{tx}(d_{ij}) \leq e_i \ \forall i \in W \quad (8)$$

Fig. 3. LP framework for lifetime maximization problem.

the discussion of bandwidth issue to Section 8 and assume here that there is plenty of bandwidth to support the rate s_i per node per unit time with a collision-free schedule.

The network consists of stationary sensor nodes in WSNs and unlike mobile adhoc networks topology changes are not frequent. Thus, topology discovery and route creation are one-time operations-for substantial amount of time (epochs) these functions are not repeated [15]. If the network reorganization period is long enough then the energy costs of these operations constitute a small fraction (less than 1%) of the total network energy dissipation [18]. Hence, routing overhead can be neglected in stationary WSNs without leading to significant underestimation of total energy dissipation.

The investigation of a lifetime optimization problem typically starts with the decision on the definition of the network lifetime. According to a common definition [3], the network lifetime is the duration between the time network starts operating and the time when the first sensor node in the network exhausts all its energy and dies. If a single node dies much sooner while the remaining nodes are left with plenty of energy then this definition of lifetime cannot capture the energy efficiency of a particular strategy. However, since the objective of MP formulations implies that the lifetime of the node that dissipates the highest amount of energy is to be maximized, all nodes collaborate to avoid the premature death of any individual node by network-wide sharing of the data forwarding burden in a balanced fashion. Therefore, we can say that this definition is a good metric that characterizes the energy efficiency of the investigated strategies.

Fig. 3 presents the formalization of lifetime maximization problem in a typical WSN with an LP model. The solution of this LP problem gives the optimal routes (network flows) between sensor nodes and the base station. The optimization objective is the maximization of t (network lifetime). Equation (5) states that all flows in the WSN are non-negative. Equation (6) is the flow balancing constraint and states that for all nodes except the base station, the amount of data flowing out of a node is equal to data flow produced and received by that node. This equation implies that the final destination of all nodes is the base station (i.e., converge-cast communication pattern). This equation also specifies a common CBR (i.e., $s_i = 240$ bits/s). Equation (7) is the maximum transmission range constraint and states that if the distance between node-i and node-j (d_{ij}) is greater than R_{max}, no data can be sent from node-i to node-j. Equation (8) is the energy constraint and states that no sensor node can spend more than its battery energy (e_i). We assume each sensor node has equal amount of energy ($e_i = e, \ \forall i \in W$) and the base station does not have

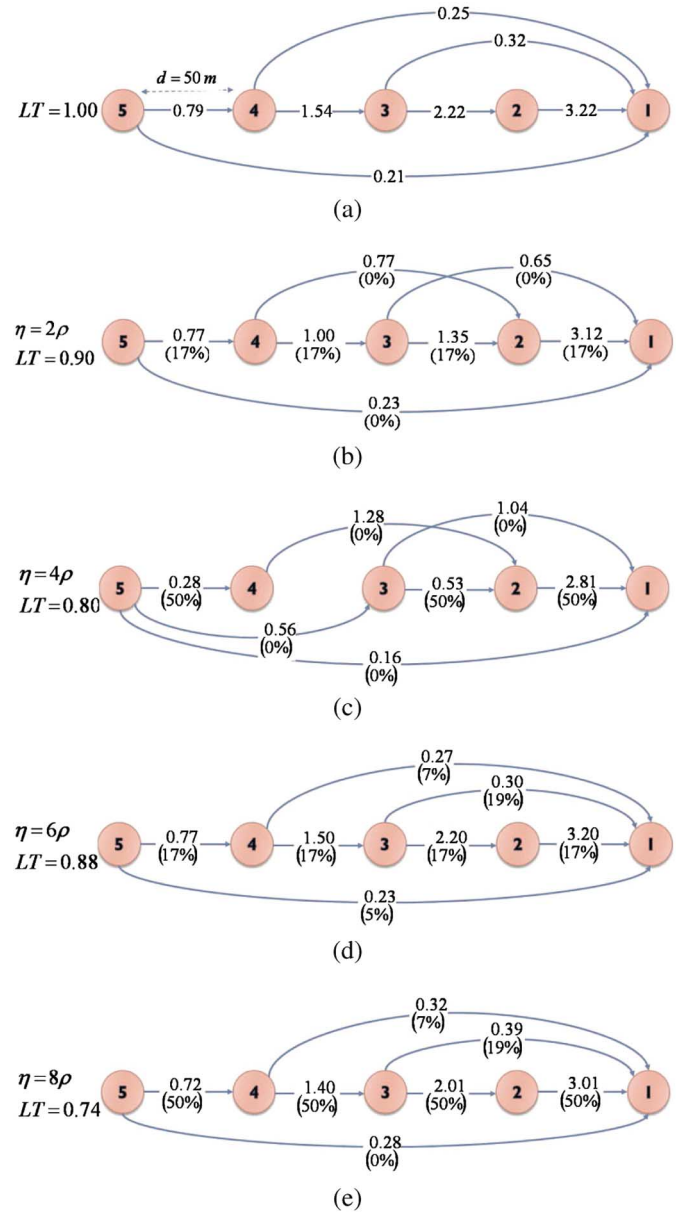

Fig. 4. Comparison of continuous and discrete *HCB* models with respect to maximum network lifetime and selected optimal routes. All lifetime (LT) values are normalized with the lifetime obtained for continuous *HCB* model used in (a). The numbers on each arc denote the amount of data flow when data generated at each node is normalized to 1. The numbers within parenthesis denote the energy dissipation overhead as a percentage when compared to perfect transmission power granularity. The values of minimum energy quantum (η) are given on the left sides of the figures.

any energy constraint. While the energy value consumed for transmitting one bit depends on the distance between source (node-i) and destination (node-j) nodes, energy consumption for receiving one bit does not. Transmission energy is calculated using the models given in Figs. 1 and 2 for continuous *HCB* model and discrete *HCB* model, respectively.

To compare continuous and discrete *HCB* models with respect to maximum network lifetime and selected optimal routes, we first employ a simple topology as shown in Fig. 4 and solve different instances of the optimization problem. We use GAMS [19] for numerical analysis of LP models. The topology consists of four sensor nodes and a base station designated as node-1, which are spaced equal-distantly on a

line. For this figure we choose $R_{max} \rightarrow \infty$ to simplify the analysis. Upon examination of Fig. 4, we can make the following remarks:

1) Independent of the minimum energy quantum value, the network lifetime obtained with continuous *HCB* model is always larger than the one obtained with discrete *HCB* model. This result is due to inequality in Equation (9) which directly follows from the definition of ceiling function. A simple intuition is that if a node is slightly beyond the reach of a discrete power level "D" then the power level needs to be increased to "D + 1" with the consequent wastage of energy.

$$\varepsilon d_{ij}^{\alpha} \leq \eta \left\lceil \frac{\varepsilon d_{ij}^{\alpha}}{\eta} \right\rceil \quad \forall \eta. \tag{9}$$

2) Generally speaking, as the minimum energy quantum value increases, the lifetime value decreases. However, there are exceptions to this general trend (lifetime value with $\eta = 6\rho$ is larger than the value with $\eta = 4\rho$). It might seem counter-intuitive to obtain a larger lifetime value with a coarser level of energy granularity. The reason underlying this result is the fact that the energy value corresponding to a larger minimum energy quantum is not always larger than the value with a smaller quantum. The distance d_{ij} is the determining factor. In other words, there can be a distance d_{ij} such that $\rho + \eta_1 \lceil \frac{\varepsilon d_{ij}^{\alpha}}{\eta_1} \rceil < \rho + \eta_2 \lceil \frac{\varepsilon d_{ij}^{\alpha}}{\eta_2} \rceil$ when $\eta_1 > \eta_2$. For example, E_{tx} values for transmissions between the adjacent nodes ($d_{ij} = 50$ m) are 7ρ and 9ρ for $\eta_1 = 6\rho$ and $\eta_1 = 4\rho$, respectively, whereas in continuous case $E_{tx} = 6\rho$. As a result, energy dissipation overheads are 50% and 17% for the transmissions between neighbor nodes in Figs. 4c and 4d, respectively.

3) We observe that replacing the continuous energy model with the discrete energy model leads to significant changes with respect to optimal network flows. Similarly, energy quantum value also has a large impact on the amount of network flows between nodes. As an example, notice that while there is no data flow from node-4 to node-2 in the continuous power case, the amount of normalized data flow between these two nodes is 0.77 when $\eta = 2\rho$. This amount increases even further to 1.28 for $\eta = 4\rho$ but reduces to zero again when $\eta = 6\rho$ and $\eta = 8\rho$. Network flows exhibit such a pattern to balance the energy dissipation of the nodes in the face of changing energy dissipation values.

To investigate the impact of discrete transmission power with different granularity levels on the network lifetime in larger networks with random node distributions, we employ a two-dimensional (2-D) topology in which nodes are deployed in a disc of radius 50 m ($R_{net} = 50$ m). All other analyses in this paper are performed on 2-D (disc shaped) topologies (the base station is located at the center and sensor nodes are distributed uniformly). Fig. 5 shows normalized lifetime as a function of minimum energy quantum (η) for different values of number of nodes (N) and maximum transmission range (R_{max}). All lifetime values are normalized with the lifetime value of the corresponding continuous power case. All data points in this figure and the other figures/tables of this paper are the averages of 1000 independent runs and in each run node positions are randomly generated. The error bars represent the standard deviations.

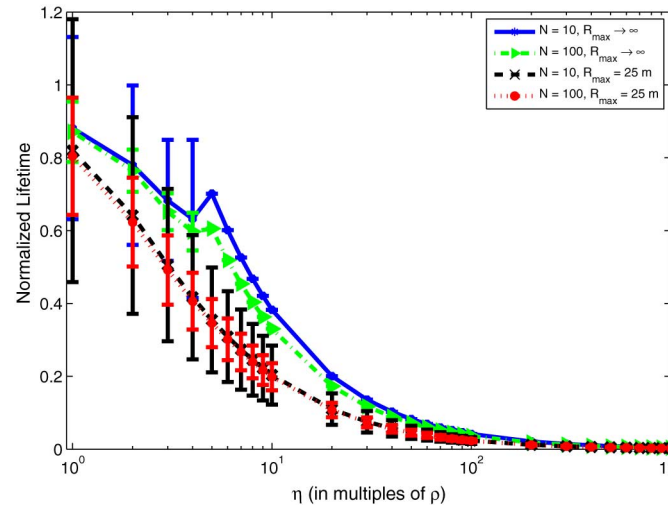

Fig. 5. Network lifetime normalized with the lifetime obtained with continuous *HCB* model as a function of η ($R_{net} = 50$ m).

Transmission range limitations may lead to disjoint partitions in the network which means that there is at least one node in the network which cannot reach the base station (neither directly nor through relaying). Disjoint partition implies that the network lifetime value is zero. We exclude runs with zero lifetime values while calculating the averages. The extent of the exclusions is at most 5% for all the data points presented in the paper. We make the following remarks on Fig. 5:

1) In denser networks (i.e., increasing N while keeping the network area constant), discretization of power levels decreases network lifetime more significantly in comparison to sparser networks. In sparse networks, average distance between the nodes is larger, hence, more transmission power is needed to send a packet to a receiver. A higher transmission power is less sensitive to discretization overhead. As an example, assume that the discrete transmission energy is always a multiple of one unit of energy. If the energy required to send to a node in close range is only half unit of energy, then the overhead due to discretization would be 100%. Compare this to the overhead for sending to a distant node requiring nine and a half units of energy. In this case, the overhead would be only 5%.
2) When range limitations are in effect, the reduction of network lifetime due to discrete power levels is more severe in comparison to corresponding $R_{max} \rightarrow \infty$ cases. The intuitive reasoning for this finding is similar to the one we present for the first remark.
3) Network lifetime decreases as η increases as a general trend. However, for a small range of η (only for $R_{max} \rightarrow \infty$) we observe a slight increase in lifetime (e.g., network lifetime slightly increases as η increases from 4 to 5) due to subtle network dynamics discussed earlier in Remark-2 on the analysis of Fig. 4.

As the final remark of this section, we note that in the discrete *HCB* energy model $\eta \rightarrow 0$ leads to a model equivalent

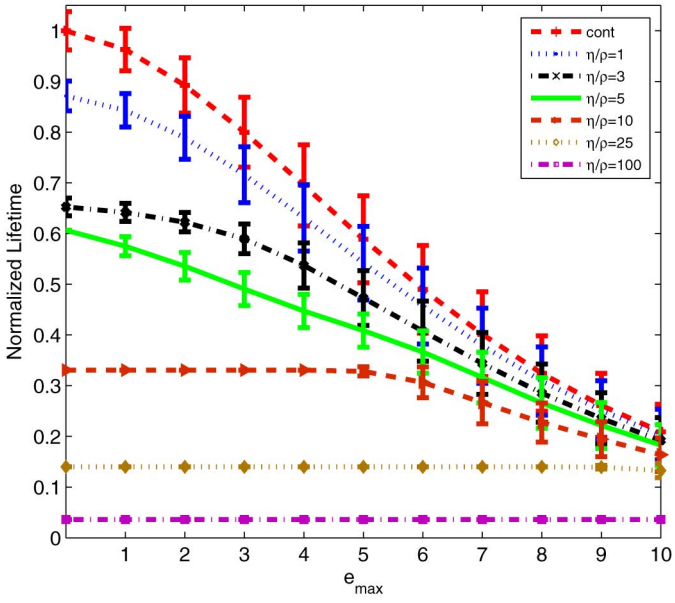

Fig. 6. Normalized lifetime as a function of positioning error for different discretization levels ($N = 100$, $R_{net} = 50$ m).

to continuous *HCB* energy model. Therefore, discrete *HCB* energy model is flexible enough to incorporate continuous *HCB* energy model as a special case.

Both the continuous and discrete HCB models evaluated in this section hold the assumption that node positions are exactly known. Since the energy dissipation value for transmission is directly related with the distance between the transmitter and the receiver in HCB models, the impact of inexact node locations on the network lifetime requires further investigation, which is done in Section 3.

3 Positioning Errors

The distance between a transmitter and a receiver cannot be measured with perfect accuracy, however, it is possible to make an estimation with a certain maximum positioning error. There exists a rich literature on position estimation in wireless networks and positioning errors up to 10 m are reported [20]-[22]. For example, positioning errors reported in [20] are below 80 cm (by using a rotatable antenna localization scheme). In [21], positioning errors in 4-9 m ranges are reported. In [22], 68% of the estimated distances have less than 1 m error, while 89% of the estimated positions are within 2 m neighborhood of the actual distances. Therefore, in this section we analyze the effects of position estimation errors in 0-10 m range.

We model positioning errors as a zero-mean uniform random distribution in $[-e_{max}, e_{max}]$ range, where e_{max} is the bound on the positioning error. If the actual distance between two nodes is d_{ij}, then the estimated distance (d^e_{ij}) is confined to the interval $[d_{ij} - e_{max}, d_{ij} + e_{max}]$. To avoid transmissions with power level lower than the actual required level due to estimation errors, we use the compensated distance (d^c_{ij}) to transmit packets. Compensated distance is obtained by $d^c_{ij} = d^e_{ij} + e_{max}$. We assume that e_{max} is known for a given network. Energy dissipation with positioning errors are modeled by replacing d_{ij}'s with d^c_{ij}'s in Figs. 1 and 2.

Normalized network lifetimes as a function of e_{max} are presented in Fig. 6 for different discretization levels along with the continuous HCB model. The following remarks are made on Fig. 6:

1) As e_{max} increases, the lifetime decreases in all cases of discretization levels. The most drastic reduction in lifetime is for the continuous case.
2) The rate of decrease is lower for higher discretization levels. For example, the lifetimes of $\eta = \rho$, $\eta = 10\rho$, and $\eta = 100\rho$ are 88%, 34%, and 3% of the continuous case for $e_{max} = 0$. On the other hand, for $e_{max} = 10$ m, the lifetimes of $\eta = \rho$, $\eta = 10\rho$, and $\eta = 100\rho$ are 97%, 69%, and 18% of the continuous case. Hence, the advantages of fine tuned transmission power adjustment decrease as the accuracy of position estimation decreases.
3) As transmission power increases to compensate for position errors, the ratio of energy waste due to discretization to the transmission energy gets smaller. In other words, the effects of increasing positioning errors are similar with decreasing node density (see Remark-1 on Fig. 5). Nevertheless, even under extreme position error conditions the finer the transmission power control is, the higher the network lifetime is.

Up to this point, in both continuous and discrete HCB energy models we assume a transmission power dependent disk shaped step function (i.e., Packet Reception Rate-PRR-is unity within a disk and is zero outside the disk). Radio irregularities are common in WSNs. With real radio chips, the radiation is not the same in all directions. Modeling radio propagation is a complex issue affected by many factors (e.g., shadowing). Thus, PRR values on links between two nodes are not binary (i.e., there is a gradual decrease in PRR). Hence, in Section 4 we modify the HCB model (both continuous and discrete cases) to incorporate the random nature of radio propagation.

4 HCB Models with Probabilistic Radio Propagation

In WSNs, quality of a link between two nodes depends on various radio and channel parameters such as path loss exponent, shadowing variance of the channel, modulation, and encoding. The log normal shadowing path loss model is shown to provide a realistic assessment of communication characteristics of WSN nodes in practice [23]. Therefore, we adopt this model and utilize the parameters presented in [23] to incorporate the propagation affects not previously considered into the HCB models.

In the log normal shadowing path loss model, the path loss $PL(d_{ij}), dB$ at a distance d_{ij} is given in dB as follows:

$$PL(d_{ij}), dB = PL(d_0), dB + 10nlog_{10}(d_{ij}/d_0) + X_\sigma, dB, \quad (10)$$

where d_{ij} is the distance between transmitter and receiver, d_0 is a reference distance, $PL(d_0), dB$ is the path loss at the reference distance in dB, n is the path loss exponent (rate at which signal decays), and X_σ, dB is a zero-mean Gaussian random variable with standard deviation σ in dB. We adopt the parameter values provided for Mica motes as $n = 4, \sigma = 4, d_0 = 1$ m, and $PL(d_0) = 55$ dB [23]. The received

signal power $P_r(d_{ij}), dB$ can be obtained by subtracting the path loss from the transmit power, $PL(d_{ij}), dB$:

$$P_r(d_{ij}), dB = P_t(d_{ij}), dB - PL(d_{ij}), dB. \quad (11)$$

In Mica motes, NRZ (Non Return to Zero) encoding and non-coherent FSK (Frequency Shift Keying) modulation is used. Therefore, probability of a successful packet reception [23] at a distance d_{ij} is:

$$PRR(d_{ij}) = \left(1 - \frac{1}{2}\exp\left(\frac{-\psi(d_{ij})}{2}\frac{1}{0.64}\right)\right)^{8\varphi}, \quad (12)$$

where $\psi(d_{ij})$ denotes signal-to-noise ratio (SNR) at a distance d_{ij} and φ is the packet size in Bytes (packet size is 30 Bytes). SNR at a distance d_{ij} is given by:

$$\psi(d_{ij}), dB = P_t(d_{ij}), dB - PL(d_{ij}), dB - P_n, dB, \quad (13)$$

where P_n, dB is the noise floor which is -145 dB at the temperature of 300 Kelvin for Mica motes [23].

We note that we do not explicitly model the effects of positioning errors in this section because the variation in path loss can be as high as an order of magnitude due to the incorporation of X_σ into the model. Thus, even with perfect position information it is not possible to estimate the actual path loss with a meaningful accuracy by using a one way estimation technique based on the actual distance between the transmitter and the receiver. Therefore, path loss should be measured by a closed loop power control mechanism [13] and we assume that such a mechanism is in effect for our model.

We incorporate probabilistic nature of radio propagation into HCB models as follows. First, we obtain the path loss values, $PL(d_{ij}), dB$, between all node pairs in the network using Equation (10). Later, we calculate SNR values by using Equation (12) for a given target PRR value. Then, by using Equation (13) we calculate the transmission power values, $P_t(d_{ij}), dB$. Conversion of dB to Watt is achieved by $P_t(d_{ij}), W = 10^{(\frac{P_t(d_{ij}), dB}{10})}$.

Energy required to transmit one bit in the continuous HCB model is modified with the log normal shadowing path loss, $E_{tx}^{C-HCB-LNS}(d_{ij})$, as follows:

$$E_{tx}(d_{ij}) = E_{tx}^{C-HCB-LNS}(d_{ij}) = \rho + \varepsilon T_b P_t(d_{ij}), W, \quad (14)$$

where T_b is the duration of a bit (52.08 μs). Likewise, the discrete HCB model is modified as follows:

$$E_{tx}(d_{ij}) = E_{tx}^{D-HCB-LNS}(d_{ij}) = \rho + \eta\left\lceil\frac{\varepsilon T_b P_t(d_{ij}), W}{\eta}\right\rceil. \quad (15)$$

Note that $E_{tx}(d_{ij})$ is the total energy dissipated at the transmitter, while $T_b P_t(d_{ij}), W$ is the energy radiated from the antenna only. In the earlier versions of HCB model, energy radiated from the antenna is modeled with d_{ij}^{α} whereas in the log normal shadowing model energy radiated form the antenna is modeled with $T_b P_t(d_{ij}), W$. Hence, unlike the original HCB model, in the log normal shadowing HCB (HCB-LNS) model path loss is not a perfect circle due to the addition of X_σ, dB (path loss over two different links with the same length can be different). Furthermore, PRR is always lower than 100% and for a given transmission power the expected value of PRR decreases with increasing transmission distance.

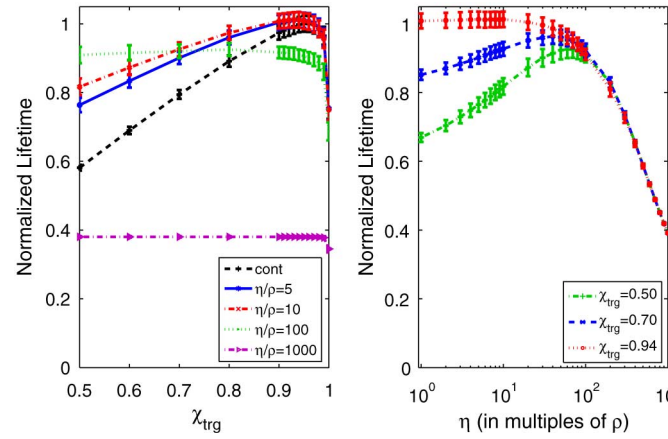

Fig. 7. Normalized lifetime as a function of PRR (left panel) and as a function of minimum energy quantum (right panel) for different discretization ratios ($N = 100$, $R_{net} = 50$ m).

To compensate for packet losses, retransmissions are required. We denote PRR value on the link from node-i to node-j as χ_{ij}. The energy cost of transmitting data packets over link (i, j) should be scaled by λ_{ij} to account for retransmissions [23]. The relation between χ_{ij} and λ_{ij} can be expressed as $\lambda_{ij} = \frac{1}{\chi_{ij}}$. For example, if $\chi_{ij} = 0.70$ then packets are transmitted 1.43 times on average ($\lambda_{ij} = 1.43$).

To account for the extra energy dissipation due to retransmissions, Equation (8) is modified as follows:

$$E_{rx}\sum_{j\in W}\lambda_{ji}f_{ji} + \sum_{j\in V}\lambda_{ij}f_{ij}E_{tx}(d_{ij}) \le e_i \;\forall i \in W. \quad (16)$$

The term λ_{ij} is used to scale both the transmission and reception energies because the receiver dissipates the same amount of energy on a failed transmission attempt (i.e., a packet should be received completely to determine whether the packet is corrupted or not).

We use the same target PRR (χ_{trg}) throughout the network. By adjusting the $E_{tx}^{C-HCB-LNS}(d_{ij})$ values we can obtain the same χ_{ij} for all links in the continuous HCB-LNS model. However, for discrete HCB-LNS model, it is not possible to obtain a constant χ_{ij} for all links due to the discretization of the transmission energy. For example, if $E_{tx}^{C-HCB-LNS}(d_{ij}) = \rho + 3.7\eta$ then $E_{tx}^{D-HCB-LNS}(d_{ij}) = \rho + 4\eta$. Therefore, the actual PRR on each link varies in discrete HCB-LNS model. In other words, for continuous HCB-LNS model $\chi_{ij} = \chi_{trg}$, while in discrete HCB-LNS model $\chi_{ij} \ge \chi_{trg}$.

In Fig. 7 (left panel), normalized network lifetime as a function of χ_{trg} is presented for continuous HCB-LNS model and discrete HCB-LNS model with $\eta = 5\rho$, $\eta = 10\rho$, $\eta = 100\rho$, and $\eta = 1000\rho$. Network lifetime reaches its maximum at $\chi_{trg} = 0.94$ for continuous HCB-LNS model. Normalization is performed by dividing all other data points by the maximum lifetime. Continuous HCB-LNS model results in lower lifetimes than discrete HCB-LNS model with $\eta = 5\rho$ and $\eta = 10\rho$ for $\chi_{trg} < 0.94$ because χ_{ij} values of discrete HCB-LNS model are higher than the suboptimal χ_{trg} due to the discretization of the transmission power as discussed previously. Fig. 7 (right panel) presents the effects of minimum

TABLE 1
Transmission Energies (μJ/bit) and Corresponding Maximum Transmission Ranges (m) in Different Power Levels (PL) of Mica Motes (Computed Using the Data Provided in [24]); Reception Energy Is Fixed ($E_{rx}^{M} = 0.922$ μJ per bit)

PL (l)	$E_{tx}^{M}(l)$	$R_{max}^{M}(l)$	PL (l)	$E_{tx}^{M}(l)$	$R_{max}^{M}(l)$
1 (l_{min})	0.672	19.30	14	0.844	41.19
2	0.688	20.46	15	0.867	43.67
3	0.703	21.69	16	1.078	46.29
4	0.706	22.69	17	1.133	49.07
5	0.711	24.38	18	1.135	52.01
6	0.724	25.84	19	1.180	55.13
7	0.727	27.39	20	1.234	58.44
8	0.742	29.03	21	1.313	61.95
9	0.758	30.78	22	1.344	65.67
10	0.773	32.62	23	1.445	69.61
11	0.789	34.58	24	1.500	73.79
12	0.813	36.66	25	1.664	78.22
13	0.828	38.86	26 (l_{max})	1.984	82.92

energy quantum on network lifetime. The following remarks are made on Fig. 7:

1) The actual operating point in discrete HCB-LNS model pushes the network towards the optimal χ_{trg} for small energy quanta.
2) For larger energy quanta (e.g., $\eta = 1000\rho$) the network lifetime is always lower than the one with continuous HCB-LNS model.
3) For the optimal χ_{trg}, the decrease in the network lifetime due to increasing minimum energy quantum is insignificant provided that the energy quantum is not too large (i.e., $\eta < 20\rho$).
4) A comparison between Figs. 5 and 7 (right panel) reveals that the network lifetime decrease due to increasing minimum energy quantum depends strongly on the path loss model utilized. For example, discrete HCB model with $\eta = 10\rho$ results in up to 80% decrease in network lifetime ($R_{max} \rightarrow \infty$ and $R_{net} = 50$ m) in comparison to continuous case, whereas with discrete HCB-LNS model ($\eta = 10\rho$) the lifetime decrease is less than 1% with the optimal target PRR.

5 Modeling Transmission Power Control Strategies

Being more practical and flexible, the extensions of the original *HCB* energy model can be useful for researchers working on different aspects of lifetime optimization problem. On the other hand, we have not yet offered concrete recommendations to practitioners who seek guidance for the issue of transmission power control in WSN applications. For this purpose, we extend our analysis by using energy dissipation values derived from experimental measurements. In this section, we explore the simple case where PRR on links between nodes are binary. In the next section, we extend our analysis using a data set which includes PRR measurements.

In this section, we use energy dissipation values and the associated transmission ranges reported in [24] using Mica motes. We refer this model as "Mica energy model" which is presented in Table 1.

We introduce various MP models formulating different transmission power control strategies. We note that these strategies [13] were already studied with respect to different performance measures [12]. Our contribution on this topic is the introduction of an MP framework under which different strategies can be compared against each other on the basis of network lifetime. Our exposition below is facilitated by first introducing various MP models using Mica energy model, and then considering the motivations of their use and analyzing the impact on network lifetime with the benefit of context from knowing their properties.

5.1 Per Network Single Level Mica Model

Per Network Single Level Mica (*PNM-SL*) model is built on the LP model in Fig. 3. The only difference is the replacement of Equation (7) and Equation (8) with Equation (17) and Equation (18), respectively. In this model, which is the simplest among all models we present, all nodes in the network transmit at a single transmission level (i.e., l_{PNM-SL}), which is a predetermined level, regardless of the distance between the source and the destination. If the distance between two nodes is higher than $R_{max}(l_{PNM-SL})$, then there cannot be a direct transmission between them.

$$f_{ij} = 0, \text{if } d_{ij} \geq R_{max}^{M}(l_{PNM-SL}) \; \forall (i,j) \in A, \tag{17}$$

$$E_{rx}^{M} \sum_{j \in W} f_{ji} + \sum_{j \in V} f_{ij} E_{tx}^{M}(l_{PNM-SL}) \leq e_i \; \forall i \in W. \tag{18}$$

5.2 Per Link Multiple Level Mica model

Per Link Multiple Level Mica (*PLM-ML*) model is also obtained by modifying the LP model in Fig. 3 by replacing Equation 7 and Equation (8) with Equation (19) and Equation (20), respectively. This model is similar to the model introduced in Section 2 which uses discrete *HCB* energy model, however, here each node chooses the optimal transmission energy from Table 1 for each link. Notice that continuous energy model is no longer an issue and transmission power is not only discrete but also takes a value from a finite set denoted as S_L (i.e., there are only 26 power levels to choose from). The optimal power level ($lopt - ij$) to transmit over a distance d_{ij} is given in Equation (21). For example, for $d_{47} = 20$ m, since $19.30 \text{ m} < d_{47} \leq 20.46$ m, node-4 uses power level 2 (l_2) to transmit data on its link to node-7 (i.e., $E_{tx}^{M}(lopt - 47) = 0.688$ μJ).

$$f_{ij} = 0, \text{if } d_{ij} > R_{max}^{M}(l_{max}) \; \forall (i,j) \in A, \tag{19}$$

$$E_{rx}^{M} \sum_{j \in W} f_{ji} + \sum_{j \in V} f_{ij} E_{tx}^{M}(lopt - ij) \leq e_i \; \forall i \in W, \tag{20}$$

$$lopt - ij = \underset{l \in S_L, d_{ij} \leq R_{max}^{M}(l)}{\arg\min} \left(E_{tx}^{M}(l) \right). \tag{21}$$

5.3 Per Network Multiple Level Mica Model

If only one power level should be chosen for a network, *PNM-SL* model described above could be solved one by one for all available power levels (i.e., $1 \leq l_{PNM-SL} \leq 26$) in order to find out which level leads to the maximum network lifetime. However if more than one power level but not all of them can be used in the network, as the number of power levels increases the aforementioned brute-force method quickly becomes intractable for finding the subset of power levels that lead to maximum lifetime. As a more efficient method, in this subsection we introduce Per Network Multiple Level Mica (*PNM-ML*) model presented in Fig. 8.

Maximize t
Subject to:

$$g_{ij}^{l} \geq 0 \ \forall l \in S_L \ \forall (i,j) \in A \quad (22)$$

$$\sum_{l \in S_L} \sum_{j \in V} g_{ij}^{l} = s_i t + \sum_{l \in S_L} \sum_{j \in W} g_{ji}^{l} \ \forall i \in W \quad (23)$$

$$g_{ij}^{l} = 0, \text{if } d_{ij} \geq R_{max}^{M}(l) \ \forall l \in S_L \ \forall (i,j) \in A \quad (24)$$

$$E_{rx}^{M} \sum_{l \in S_L} \sum_{j \in W} g_{ji}^{l} + \sum_{l \in S_L} \sum_{j \in V} g_{ij}^{l} E_{tx}^{M}(l) \leq e_i \ \forall i \in W \quad (25)$$

$$\sum_{i \in W} \sum_{j \in V} g_{ij}^{l} = h^{l} \ \forall l \in S_L \quad (26)$$

$$h^{l} \leq M a^{l} \ \forall l \in S_L \quad (27)$$

$$\sum_{l \in S_L} a^{l} \leq L_{PNM-ML} \quad (28)$$

Fig. 8. MIP framework for *PNM-ML* model.

For *PNM-ML* model and *PSM-ML* model (introduced in subsection 5-D), instead of f_{ij} we employ the notation g_{ij}^{l} which represents the flow from node-i to node-j at power level l. The third argument (l) is needed in order to incorporate all possible power levels into the flow balancing constraint given in equation (23). However, the last three equations in Fig. 8 restrict the number of power levels used (L_{PNM-ML}). Equation (26) adds up all flows pertaining to a single level. Equation (27) separates power levels into two groups (the binary variable a_l takes the value of 1 if there is a nonzero flow using power level l, and the value of 0 otherwise). Equation (28) counts the number of power levels used and puts an upper limit for it. We note that instead of *PNM-SL* model we can alternatively use *PNM-ML* model to find the optimal static (single) power level by setting L_{PNM-ML} to 1.

5.4 Per Sensor Multiple Level Mica Model

The formulation of Per Sensor Multiple Level Mica (*PSM-ML*) model is very similar to the *PNM-ML* model in Fig. 8. The only difference is that instead of putting a limit that specifies global power levels for all nodes, a limit on the number of power levels is applied for each individual node, separately (i.e., Equation (26), Equation (27), and Equation (28) are replaced with Equation (29), Equation (30), and Equation (31), respectively). This means different nodes in the network can be adjusted with different power levels as long as the total number per node does not exceed a maximum value. For the case when L_{PSM-ML} is set to maximum (i.e., 26), this model is equivalent to *PLM-ML* model.

$$\sum_{j \in V} g_{ij}^{l} = h_i^{l} \ \forall i \in W, \ \forall l \in S_L, \quad (29)$$

$$h_i^{l} \leq M a_i^{l} \ \forall i \in W \ \forall l \in S_L, \quad (30)$$

$$\sum_{l \in S_L} a_i^{l} \leq L_{PSM-ML} \ \forall i \in W. \quad (31)$$

6 Transmission Power Control Strategies in the Presence of Packet Losses

In Section 5, we present MP models based on the data presented in [24], which provides transmission power levels and corresponding maximum transmission ranges. However, in practice the transmission range for a given power level cannot be so sharp (i.e., there should be a transition range where bit error rate is between 0% and 100%). One option to incorporate packet errors is using the modeling approach presented in Section 4. However, since in Section 5 we start building our models on an experimental energy dissipation data set, in this section we opt to extend our model to include packet reception errors by using the experimental data presented in [25]. We refer this energy model as "Mica energy model with packet loss" (Mica-PL). In [25], eight power levels of Mica motes are used. Power levels 1, 2, 3, 4, 5, 6, 7, and 8 used in this study correspond to power levels 1, 6, 11, 14, 16, 18, 20, and 21, respectively, in Table 1. We denote the set of power levels having only these eight levels as S_{PL}. For each power level, PRR is measured in five meter increments of the distance between the transmitter and the receiver up to 65 m. Therefore, packet reception rates (χ_{lk}^{M}) are reported for 13 different d_k distances ($d_1 = 5$ m and $d_{13} = 65$ m) for each of the eight transmission power levels, presented in Table 2). We note that measurements were performed in a fairly flat open grassy field, yet, the existence of some degree of unevenness in the terrain (e.g., a slight hill at 30-35 meters) manifested itself as irregularities in the data (e.g., $\chi_{66}^{M} > \chi_{67}^{M}$). Nevertheless, the general trend in the data is consistent with expectations (i.e., packet reception rate decreases with range and higher power levels have higher packet reception rates than lower power levels at the same range). As explained in Section 4, to compensate for packet losses flows should be scaled with $\lambda_{lk}^{M} = \frac{1}{\chi_{lk}^{M}}$. In the following subsections, we present the modified versions of the four MP models introduced in Section 5 to utilize the Mica-PL energy model.

TABLE 2
Mica-PL Energy Model Packet Reception Rates (χ_{lk}^{M}) as Functions of d_k (m) and Power Level (PL)

d_k	PL-1	PL-2	PL-3	PL-4	PL-5	PL-6	PL-7	PL-8
5	1.0	1.0	1.0	1.0	1.0	1.0	1.0	1.0
10	1.0	1.0	1.0	1.0	1.0	1.0	1.0	1.0
15	0.0	1.0	1.0	1.0	1.0	1.0	1.0	1.0
20	0.0	0.3	1.0	1.0	1.0	1.0	1.0	1.0
25	0.0	0.0	1.0	1.0	1.0	1.0	1.0	1.0
30	0.0	0.0	0.8	1.0	1.0	1.0	1.0	1.0
35	0.0	0.0	0.0	0.4	0.9	0.8	0.6	0.9
40	0.0	0.0	0.0	0.5	0.7	1.0	1.0	1.0
45	0.0	0.0	0.0	1.0	1.0	1.0	1.0	1.0
50	0.0	0.0	0.0	0.8	0.6	1.0	1.0	1.0
55	0.0	0.0	0.0	0.0	0.7	1.0	1.0	1.0
60	0.0	0.0	0.0	0.0	0.4	1.0	1.0	1.0
65	0.0	0.0	0.0	0.0	0.0	0.3	0.7	0.3

6.1 Per Network Single Level Mica Model with Packet Loss

Per Network Single Level Mica model with Packet Loss (*PNM-SL-PL*) is constructed using the LP model in Fig. 3. However, Equation (7) and Equation (8) are replaced with Equation (32) and Equation (33), respectively. The maximum transmission range (R_{max}^{M-PL}) is 65 m and $\widehat{d_{ji}} = 5 \times \lceil \frac{d_{ji}}{5} \rceil$.

$$f_{ij} = 0, \text{if } d_{ij} > R_{max}^{M-PL} \ \forall (i,j) \in A, \quad (32)$$

$$E_{rx}^{M} \sum_{j \in W} \lambda_{l_{PNM-SL}, \widehat{d_{ij}}}^{M} f_{ji} + \sum_{j \in V} \lambda_{l_{PNM-SL}, \widehat{d_{ji}}}^{M} f_{ij} E_{tx}^{M}(l_{PNM-SL}) \leq e_i \ \forall i \in W. \quad (33)$$

6.2 Per Link Multiple Level Mica Model with Packet Loss

Per Link Multiple Level Mica model with Packet Loss (*PLM-ML-PL*) is very similar to *PNM-SL-PL* model. The only difference is the replacement of Equation (33) with Equation (34). The optimal power level to be used in Mica-PL model for transmission from node-i to node-j ($loptPL-ij$) is found by Equation (35).

$$E_{rx}^{M}\sum_{j\in W}\lambda_{loptPL-ji,\widehat{d_{ji}}}^{M}f_{ji}+ \sum_{j\in V}\lambda_{loptPL-ij,\widehat{d_{ij}}}^{M}f_{ij}E_{tx}^{M}(loptPL-ij)\leq e_i\ \forall i\in W, \quad (34)$$

$$loptPL-ij=\arg\min_{l\in S_{PL}}\left(E_{tx}^{M}(l)\lambda_{l,\widehat{d_{ij}}}^{M}\right). \quad (35)$$

6.3 Per Network Multiple Level Mica Model with Packet Loss

Per Network Multiple Level Mica model with Packet Loss (*PNM-ML-PL*) is built on the *PNM-ML* model (Section 5-C). The difference is the replacement of equations from Equation (24) to Equation (28) with Equation (36) to Equation (40).

$$g_{ij}^{l}=0, \text{if } d_{ij}>R_{max}^{M-PL}\ \forall l\in S_{PL}\ \forall (i,j)\in A, \quad (36)$$

$$E_{rx}^{M}\sum_{l\in S_{PL}}\sum_{j\in W}\lambda_{l,\widehat{d_{ij}}}^{M}g_{ji}^{l}+ \sum_{l\in S_{PL}}\sum_{j\in V}\lambda_{l,\widehat{d_{ij}}}^{M}g_{ij}^{l}E_{tx}^{M}(l)\leq e_i\ \forall i\in W, \quad (37)$$

$$\sum_{i\in W}\sum_{j\in V}g_{ij}^{l}=h^{l}\ \forall l\in S_{PL}, \quad (38)$$

$$h^{l}\leq Ma^{l}\ \forall l\in S_{PL}, \quad (39)$$

$$\sum_{l\in S_{PL}}a^{l}\leq L_{PNM-ML}. \quad (40)$$

6.4 Per Sensor Multiple Level Mica Model with Packet Loss

Per Sensor Multiple Level Mica model with Packet Loss (*PSM-ML-PL*) is obtained by modifying the *PNM-SL-PL* model. Equation (38), Equation (39), and Equation (40) are replaced with Equation (41), Equation (42), and Equation (43), respectively.

$$\sum_{j\in V}g_{ij}^{l}=h_{i}^{l}\ \forall i\in W,\ \forall l\in S_{PL}, \quad (41)$$

$$h_{i}^{l}\leq Ma_{i}^{l}\ \forall i\in W,\ \forall l\in S_{PL}, \quad (42)$$

$$\sum_{l\in S_{PL}}a_{i}^{l}\leq L_{PSM-ML}\ \forall i\in W. \quad (43)$$

7 Analysis of Transmission Power Control Strategies

In Section 5 and Section 6, we introduce a family of MP models formulating different power control strategies. In this section, we present the results of our numerical analysis to characterize these strategies with respect to their impact on network lifetime.

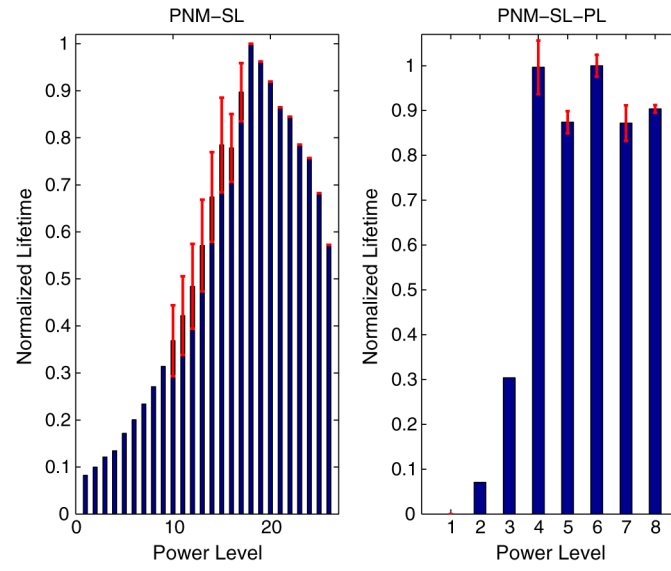

Fig. 9. Normalized lifetime with *PNM-SL* (left panel) *PNM-SL-PL* (right panel) with $N=50$, $R_{net}=50$ m.

First of all, we are interested in the following question. If the same single power level is assigned to all nodes, then which power level leads to the maximum network lifetime? Fig. 9 present normalized network lifetimes using *PNM-SL* model and *PNM-SL-PL* model. The analysis is performed with 50 nodes and 50 m of radius. The maximum lifetime for *PNM-SL* model is obtained when power level is set to 18. The lifetime with the first power level ($l_{PNM-SL}=1$) is only 8% and with the last level ($l_{PNM-SL}=26$) is 57% of the maximum lifetime. For *PNM-SL-PL* model, lifetime is maximized at power level 6, which corresponds to power level 18 in Table 1. Hence, both models show that neither the minimum nor the maximum power level can maximize the network lifetime. Using the maximum power level wastes energy since the base station is within the distance of at most 50 m to all nodes, hence, could be reached using lower power levels whereas multi-hop forwarding over a relay node using minimal power level is not more energy-efficient than a longer-range direct transmission when the energy values given in the data sets are used. As a result, an intermediate power level is the optimal for maximizing network lifetime.

In Fig. 10, the power levels corresponding to maximum lifetime values are presented for *PNM-SL* model and *PNM-SL-PL* model, as functions of R_{net} for $N=50$, $N=70$, and $N=100$. When the number of nodes in the network is kept constant, the power level which maximizes the network lifetime changes significantly as a function of network radius in both models (i.e., the general trend is to utilize higher power levels in larger area networks). Varying the number of nodes does not have a significant impact on the power level maximizing the network lifetime because the optimal choice is always to send to the farthest node possible with the available power level. In other words, more options for multi-hop forwarding is not much of a use when there is only one power level.

Fig. 9 shows that when the power levels are set to their maximum values, there are lifetime reductions of 43% (*PNM-SL*) and 11% (*PNM-SL-PL*) as compared to the cases of optimal power level. These results suggest that use of

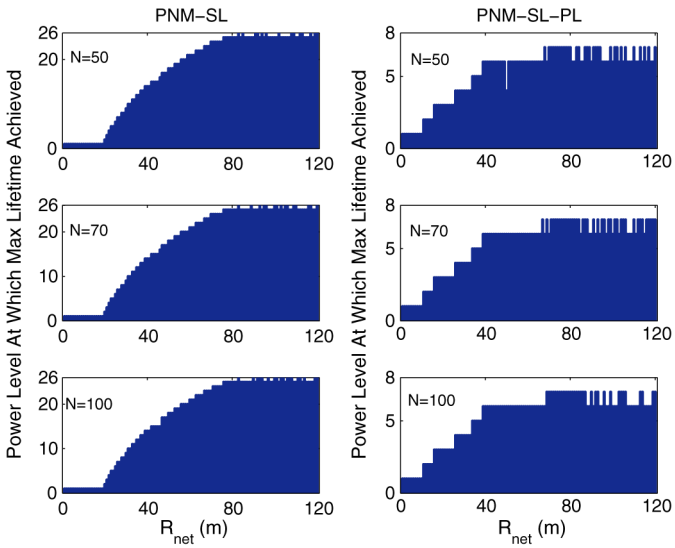

Fig. 10. Power level at which maximum lifetime achieved *PNM-SL* (left panel) and *PNM-SL-PL* (right panel) as a function of R_{net}.

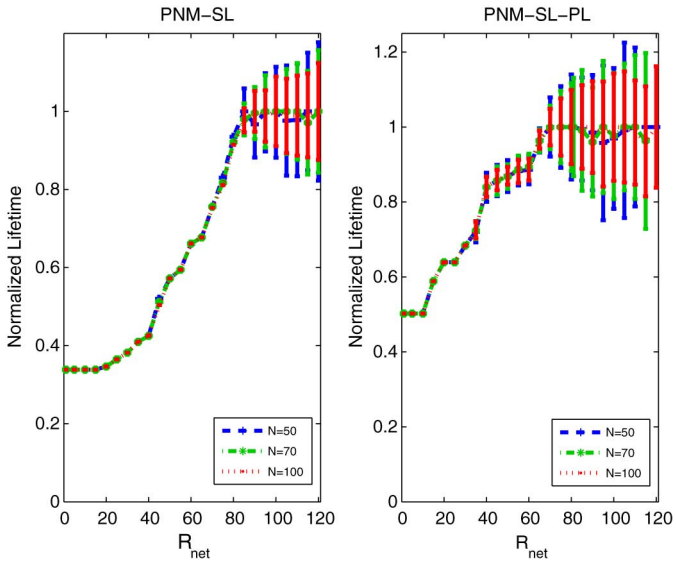

Fig. 11. Normalized lifetime at maximum power level for *PNM-SL* (left panel) and *PNM-SL-PL* (right panel).

maximum power level is a better (but still not the best) choice when packet losses are taken into consideration. On the other hand, an analysis performed by using a single parameter set is not sufficient for characterization. Hence, to investigate the effects of assigning power level to its maximal value with a larger parameter set, another analysis is performed with different number of nodes and radii. Fig. 11 present normalized lifetimes for the power level 26 (Mica energy model) and for the power level 8 (Mica-PL energy model) as functions of R_{net} for $N = 50$, $N = 70$, and $N = 100$. The lifetime of maximum power level is normalized with the maximum lifetime associated with R_{net} and N values. Number of nodes do not have a significant impact on the lifetime in networks with sufficiently high number of nodes. Network radius is the determining factor in the performance of maximum power level with respect to the network lifetime. For smaller radii, utilization of maximal power level results in poor network

TABLE 3
Comparison of Transmission Power Assignment Strategies with Respect to Network Lifetime ($N = 50$, $R_{net} = 50$ m)

Strategy	Normalized Lifetime
PNM-SL ($l_{PNM-SL} = 18$)	0.86 ± 0.00
PSM-ML ($L_{PSM-ML} = 1$)	0.88 ± 0.08
PLM-ML	1.00 ± 0.10
PNM-SL-PL ($l_{PNM-SL} = 6$)	0.83 ± 0.10
PSM-ML-PL ($L_{PSM-ML} = 1$)	0.93 ± 0.05
PLM-ML-PL	1.00 ± 0.05

lifetime performances. For example, network lifetimes obtained using the highest power levels with Mica energy model and Mica-PL energy model are one third and one half of the network lifetimes obtained with optimal power levels, respectively when $R_{net} = 10$ m. On the other hand, for larger network radii employing maximum power levels leads to network lifetimes in close proximity of the maximal lifetimes obtained with optimal power levels. For example, in larger networks ($R_{net} \geq 80$ m) normalized lifetime values obtained with maximum power level assignment are always within 4% and 8% of the maximum network lifetime for Mica energy model and Mica-PL energy model, respectively. So, with a sufficiently large network radius maximum power level is a feasible alternative to optimal power level with a fairly insignificant lifetime sacrifice.

Up to this point, our analysis is on optimizing lifetime when a single power level is used throughout the whole network. Network lifetime can be further increased by two more sophisticated strategies.

In the first of these strategies (i.e., *PSM-ML*$-L_{PSM-ML} = 1$), the same power level is not used in all nodes but instead we select the power level optimally for each node depending on its location. In other words, the power level is assigned not per network but per node. Note that there is still a single power level used by each node.

The second strategy (i.e., *PLM-ML*) is even more fine-grained (i.e., choose the power level not per node but per link). Here, given a flow to a destination node, each node chooses the optimal power level that minimizes the energy consumption.

In Table 3, a comparison of assigning a single power level per network optimally (i.e., *PNM-SL* and *PNM-SL-PL*), assigning a single power level per node optimally (*PSM-ML* and *PSM-ML-PL* with $L_{PSM-ML} = 1$) and assigning power levels per link optimally (*PLM-ML* and *PLM-ML*) is presented for a 50-node network having a radius of 50 meters. In $x \pm y$ notation, x and y represent the mean and the standard deviation of an ensemble, respectively. Network lifetime values are normalized with those of *PLM-ML* and *PLM-ML-PL*.

Network lifetimes obtained using *PSM-ML* and *PSM-ML-PL* (with $L_{PSM-ML} = 1$) are 2% and 12% more that the network lifetimes obtained using *PNM-SL* and *PNM-SL-PL*, respectively. *PLM-ML* and *PLM-ML-PL* increase the lifetimes by 16% and 20% in comparison to the lifetimes obtained using *PNM-SL* and *PNM-SL-PL*, respectively. These results are not in contradiction with the expectation that more fine-grained transmission power control leads to a larger network lifetime.

In Table 4, the impact of number of power levels in network-level and node-level strategies is presented.

TABLE 4
Normalized Lifetimes for L_{PNM-ML} and L_{PSM-ML} (Both Are Referred to as L_x in the Table) with $N = 50$, $R_{net} = 50$ m

L_x	*PNM-ML*	*PNM-ML-PL*	*PSM-ML*	*PSM-ML-PL*
1	0.84 ± 0.08	0.84 ± 0.11	0.89 ± 0.10	0.93 ± 0.03
2	0.89 ± 0.10	0.95 ± 0.07	0.96 ± 0.11	0.95 ± 0.06
4	0.94 ± 0.09	0.97 ± 0.08	1.00 ± 0.14	0.96 ± 0.08
8	0.97 ± 0.10	1.00 ± 0.06	1.00 ± 0.10	1.00 ± 0.06
16	0.99 ± 0.11	–	1.00 ± 0.09	–
26	1.00 ± 0.09	–	1.00 ± 0.09	–

Normalized network lifetimes are presented as functions of L_{PNM-ML} and L_{PSM-ML}, respectively. For *PNM-ML* and *PNM-ML-PL*, all available power levels are needed to obtain the maximum network lifetime, hence, using a subset of all available power levels leads to a suboptimal energy dissipation characteristics. Yet, for *PNM-ML* with $L_{PNM-ML} = 8$ and $L_{PNM-ML} = 16$, normalized network lifetimes are 0.97 and 0.99, respectively. Therefore, using a reduced subset with $L_{PSM-ML} \geq 8$ of all available power levels is a viable option if a small decrease (2%) in network lifetime is acceptable. Likewise, for *PNM-ML-PL* network lifetime decrease is at most 5% for $L_{PNM-ML} \geq 2$. For *PSM-ML*, maximum network lifetime can be achieved by using only four power levels for each node. However, for *PSM-ML-PL* all power levels need to be utilized to achieve the maximum lifetime. Nevertheless, for both *PSM-ML* and *PSM-ML-PL* lifetime decrease is at most 5% for $L_{PSM-ML} \geq 2$.

8 Bandwidth Requirements

In previous sections, we focus on lifetime optimization problem and do not consider bandwidth requirements of the aforementioned power control strategies. Without any constraint on bandwidth, the data rate parameter (i.e., a common CBR of $s_i = 240$ bits/s) has no influence on normalized lifetimes, which are ratios between two lifetime values. Since more bandwidth is needed as source data rate increases, our analysis on bandwidth requirements helps us to answer two related questions for each of the power control strategies:

1) Would the bandwidth (data rate) of Mica motes (38.4 Kbps) be sufficient to support the data rate of 240 bits/s per node?
2) What would be the maximum common CBR that can be supported on Mica motes?

To investigate the effects of bandwidth limitations on network lifetime, our first step is to determine the interfering flows. Equation (44) states that node-j's transmission at power level l interferes with node-i if the maximum transmission range at power level l times γ is greater than or equal to the distance between node-i and node-j. $\gamma \geq 1$ represents the interference factor of the transmission environment. Note that the node's own incoming and outgoing flows are not included in the interfering flows of the node.

$$I_{jl}^{i} = \begin{cases} 1, & \text{if } \gamma R_{max}^{M}(l) \geq d_{ij} \text{ and i } \neq \text{ j}, \\ 0, & \text{else.} \end{cases} \tag{44}$$

Equation (45) is the generic form of the bandwidth constraint that is used to incorporate the bandwidth limitations into the MP models based on Mica energy model (Section 5).

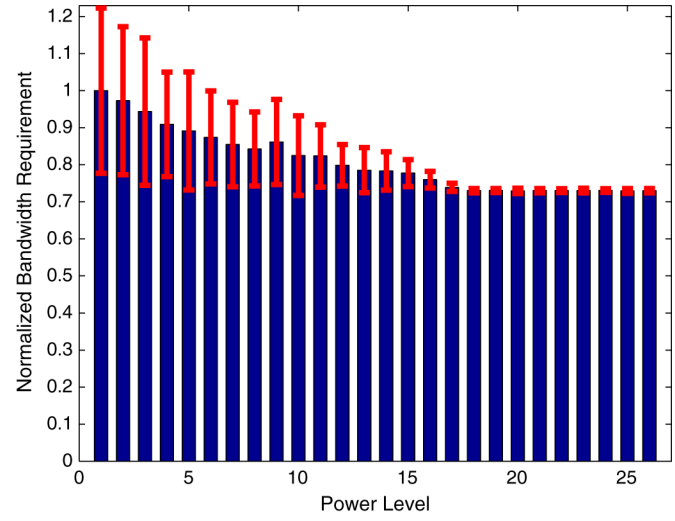

Fig. 12. Bandwidth requirement for each power level to achieve maximum lifetime for *PNM-SL* ($N = 50$, $R_{net} = 50$ m, $\gamma = 1.7$).

The sum of total amount of incoming, outgoing, and interfering flows of each node must be less than or equal to available bandwidth B multiplied with network lifetime t. This is a modified version of the sufficient condition formalized and proved in [17]. We use a generic flow variable x_{ij}^{l} to represent the bandwidth constraint for all MP models presented in Section 5 with a single equation. For *PNM-SL*, x_{ij}^{l} is replaced with f_{ij}, summations over l are removed, and $l = l_{PNM-SL}$. The only difference in *PLM-ML* bandwidth constraint than *PNM-SL* is that $l = lopt - jk$. For both *PNM-ML* and *PSM-ML* models, x_{ij}^{l} is replaced with g_{ij}^{l}.

$$\sum_{l \in S_L} \sum_{j \in W} x_{ji}^{l} + \sum_{l \in S_L} \sum_{j \in V} x_{ij}^{l} + \sum_{l \in S_L} \sum_{j \in W} \sum_{k \in V} x_{jk}^{l} I_{jl}^{i} \leq B \times t \; \forall i \in V. \tag{45}$$

Equation (46) is the generic form of the bandwidth constraint that takes into account the extra bandwidth required due to retransmissions in the MP models based on Mica-PL energy model (Section 6), where λ_{ij}^{l} is a generic flow scaling variable. For *PNM-SL-PL*, x_{ij}^{l} is replaced with f_{ij}, summations over l are removed, $l = l_{PNM-SL}$, and $\lambda_{ij}^{l} = \lambda^{M}_{l_{PNM-SL}, \widehat{d_{ij}}}$. *PLM-ML-PL* differs from *PNM-SL-PL* by the power level index ($l = loptPL - jk$). For both *PNM-ML-PL* and *PSM-ML-PL* models, x_{ij}^{l} is replaced with g_{ij}^{l} and $\lambda_{ij}^{l} = \lambda^{M}_{l, \widehat{d_{ij}}}$.

$$\sum_{l \in S_L} \sum_{j \in W} \lambda_{ji}^{l} x_{ji}^{l} + \sum_{l \in S_L} \sum_{j \in V} \lambda_{ij}^{l} x_{ij}^{l} + \sum_{l \in S_L} \sum_{j \in W} \sum_{k \in V} \lambda_{jk}^{l} x_{jk}^{l} I_{jl}^{i} \leq B \times t \; \forall i \in V. \tag{46}$$

To determine the bandwidth requirements of power control strategies we first assign a large enough B value so that bandwidth constraint does not have an effect on the network lifetime. Then, we start reducing it till the point where the lifetime value starts decreasing (due to suboptimal network flows enforced by the bandwidth constraint). The value of the bandwidth for which the lifetime starts decreasing is the minimum bandwidth requirement. Fig. 12 shows the normalized minimum bandwidth requirement of each power level

TABLE 5
Comparison of Power Level Assignment Strategies with Respect to Bandwidth Requirement ($N = 50$, $R_{net} = 50$ m, $\gamma = 1.7$)

Strategy	Normalized Bandwidth Requirement
PNM-SL ($l_{PNM-SL} = 18$)	0.75 ± 0.03
PSM-ML ($L_{PSM-ML} = 1$)	0.78 ± 0.04
PLM-ML	1.00 ± 0.43
PNM-SL-PL ($l_{PNM-SL} = 6$)	0.99 ± 0.07
PSM-ML-PL ($L_{PSM-ML} = 1$)	1.00 ± 0.07
PLM-ML-PL	1.00 ± 0.06

for *PNM-SL* model. The largest bandwidth requirement is observed for the lowest power level which also has the lowest network lifetime (see also Fig. 9). As the power level increases, the bandwidth requirement decreases. The difference between the maximum bandwidth demand (power level 1) and the minimum bandwidth demand (power level 26) is less than 30%.

We also perform a similar analysis for *PNM-SL-PL* model. Although, the general trend is the same in the sense that lower power levels require more bandwidth, the difference between the maximum and the minimum bandwidth demands is less than 20%. We attribute this difference to the presence of retransmissions. Bandwidth requirements increase with retransmissions which are in general required more frequently when higher power levels are used.

To understand the network dynamics of bandwidth requirements and to see why lower power levels require higher bandwidths, consider a small WSN consisting of three nodes placed on a line, where node-1 is the base station, node-2 is 10 m away from node-1, and node-3 is 10 m away from node-2. Both node-2 and node-3 generates one unit of data per unit time to be transferred to the base station. If each node has a maximum transmission range of 10 m, then the minimum bandwidth to transfer all data to node-1 cannot be lower than three data units per unit time (i.e., three transmissions of one data unit which cannot be concurrent are needed). If each node has a transmission range of 20 m, then the bandwidth requirement can be as low as two data units per unit time (i.e., both node-2 and node-3 can transmit their data directly to the base station).

In Table 5, a comparison of bandwidth requirements of transmission power control strategies are presented. For Mica energy model, link-level power control (PLM-ML) leads to an increased bandwidth requirement. The simple topology with 3-nodes discussed above may also help us to understand the reason here. Suppose node-3 has two power levels, one has a transmission range of 10 m and the other has 20 m. Then, for energy balancing reasons, node-3 transfers some of its data to node-2 using the first power level and some of its data directly to the base station using the second level. As a result, the bandwidth requirement is higher than two but lower than three data units per unit time. For Mica-PL energy model, the same reasoning does not hold due to existence of retransmissions which also affect the bandwidth requirements as previously described.

We now return to the questions posed at the beginning of this section. Bandwidth requirements depend on the power control strategy, energy model, data generation rate (s_i), number of nodes (N), power level (l) and radius (R_{net}). For example, in *PNM-SL* model if $N = 50$, $R_{net} = 50$ m, $l_{PNM-SL} = 18$, and $s_i = 768$ bits then the required bandwidth is 38.4 Kbps. So, Mica data rate is sufficiently high if $s_i = 240$ bits/second (a reduction in network lifetime due to low bandwidth is not happening). In fact, the data generation rate used ($s_i = 240$ bits/second) is low enough to avoid a decrease in network lifetime for all strategies and the whole parameter space explored in the paper with Mica data rate of 38.4 Kbps. Hence, the results presented in Section 7 are not affected from the bandwidth constraint presented in Equation (45) and Equation (46). Table 5 could help us to answer our second question (the maximum common CBR that can be supported on Mica motes) for different strategies. For instance, with *PLM-ML* model, the maximum data rate is $s_i = 576$ bits/second which is 25% less than the maximum data rate possible with *PNM-SL* model.

9 Related Work

Heinzelman, Chandrakasan, and Balakrishnan [15] proposed a radio model in which transmission power can be adjusted in a continuum depending on the distance between the transmitter and the receiver. Since many later studies adopted it, in our work we revisit this model and introduce modifications in order to investigate the impact of discretization and its granularity on the network lifetime.

Our study is not the first in employing a discrete power level model. A useful taxonomy of earlier work could be found in [13] where network-level, node-level and neighbor (link) level categories were identified.

Although the literature is rich, all previous studies addressed the issue of transmission power control in rather different contexts. For instance, in [13], a lightweight algorithm of adaptive (link-level) transmission power control for WSN was presented. The design was guided by field experiments performed over a long period of time. One of the main conclusions is that more energy savings could be achieved with a more fine-tuned control capability (their solution consumes 53.6% of the transmission energy of the maximum power solution and 78.8% of the transmission energy of the network-level optimal solution). In our work, we reach the same conclusion but using a different framework. Rather than designing a specific algorithm, we choose an analysis method abstracted away from implementation details.

Another adaptive algorithm supported with an empirical study was proposed in [26] which is designed to minimize the transmission power of a link without violating the user-specified PRR bound. It is interesting to notice that the target PRR of 0.95 in this work is close to the PRR value of 0.94, which we found to be the optimal target in our analysis.

There are other experimental studies on the topic of discrete power levels. We use the data reported in two of these [24], [25]. There are also many simulation based studies that investigate the topic of transmission power control [12].

In [27], the importance of selecting a proper radio model for the problem of WSN lifetime estimation was investigated. In [28], cluster-based communication of WSNs was analyzed. It was shown that the discrete power model can affect the system behavior dramatically in comparison with the results obtained under ideal conditions. Clustering protocols including LEACH [15] and others were modified by incorporating a discrete model compliant with Mica motes [29].

Several studies (e.g., [11]) proposed algorithms that find the appropriate transmission power in order to hold the number of neighbors within a desired range. Connectivity based, packet reception rate based, and received-signal strength based neighbor selection policies were analyzed with respect to their effects on the necessary transmission power.

MP is a powerful tool utilized in many studies to analyze different aspects of WSNs [3]-[5]. However, up to our best knowledge, there is only one previous study which investigates the issue of discrete power levels in WSNs through an MP framework. In [30], a novel model was proposed where a minimum transmission range and corresponding transmission power is assumed to be given and all power levels can be set as only the multiples of the minimum transmission power. Using this energy model and dividing the network into different layers depending on the distances to the base station it was shown that optimum solution is to send traffic either to an inner layer or to the base station directly (assuming that each node can reach the base station directly).

10 Conclusion

In this study, we investigate the impact of transmission power control using discrete power levels on both network lifetime and bandwidth requirements. Unlike earlier work which either were simulation-based or contributed to the area by designing a specific power control algorithm, we develop a family of mathematical programming models to explore the impact of transmission power granularity and to compare the performances of various discrete transmission power assignment strategies. This approach gives us the opportunity to perform numerical analysis spanning a wide range of parameters. Since the motivation for this paper is provided in the form of a series of questions in Section 1, we present our main conclusions in reply to these questions itemized as follows:

1) We observe that network lifetime decreasing with increasing energy quantum is the general trend. Particularly for large minimum energy quantum values ($\eta > 100\rho$), discretization of transmission power has a significant impact on network lifetime. However the exact characteristics strictly depend on the adopted path loss model. We observe smaller decreases if log normal path shadowing model is used. With this model, packet reception rates are incorporated into the model. As a result, extra power dissipated due to discretization is not wasted, instead it may help to increase the reception rate, which leads to less re-transmissions and less energy overhead. This phenomena is more evident when the target packet reception rate is chosen below the optimal value. If this is the case, up to a certain energy quantum value discretization may even yield a lifetime value higher than the one achieved with continuous model. We also note that as transmission power increases to compensate for the position errors, the impact of granularity on network lifetime becomes less important.
2) Utilizing all available power levels might be necessary to avoid any impact on network lifetime. However, a subset with more than two power levels could be used if a lifetime decrease up to 5% is tolerable.
3) If transmission power levels could be adjusted per link, then the achievable network lifetime could be higher than the case where a single level is assigned to each node optimally (e.g., roughly, 10% increase in lifetime).
4) When a single power level is optimally assigned per node rather than an optimal network-wide assignment, for Mica energy model, the lifetime improvement is marginal (i.e., 2%). However, for Mica energy model with packet loss, more significant lifetime gains can be achieved (i.e., 10%).
5) With relatively larger network sizes ($R_{net} \geq 80$ m), normalized network lifetime values obtained for the maximum power level are always within 8% of the maximum network lifetime possible with any other single power level, hence, for large area networks with sufficiently high node density, utilization of the maximum power level instead of searching for the optimal power level is a feasible option which does not deteriorate network lifetime significantly.
6) When a single level is used, bandwidth requirements decrease with increasing power levels. Comparison to other strategies also reveals that more fine-grained strategies increase the bandwidth requirements. This increase is modest which results in at most 25% reduction to the maximum common constant bit rate that can be carried in the network without a penalty in terms of lifetime.

References

[1] G. Anastasi, M. Conti, M.D. Francesco, and A. Passarella, "Energy Conservation in Wireless Sensor Networks: A Survey," *Ad Hoc Networks*, vol. 7, pp. 537-568, 2009.

[2] K. Akkaya and M. Younis, "A Survey on Routing Protocols for Wireless Sensor Networks," *Ad Hoc Networks*, vol. 3, pp. 325-349, 2005.

[3] Z. Cheng, M. Perillo, and W. Heinzelman, "General Network Lifetime and Cost Models for Evaluating Sensor Network Deployment Strategies," *IEEE Trans. Mobile Computing*, vol. 7, pp. 484-497, Apr. 2008.

[4] J.H. Chang and L. Tassiulas, "Maximum Lifetime Routing in Wireless Sensor Networks," *IEEE/ACM Trans. Networking*, vol. 12, pp. 609-619, Aug. 2004.

[5] M. Bhardwaj and A. Chandrakasan, "Bounding the Lifetime of Sensor Networks via Optimal Role Assignments," *Proc. 21st Ann. Joint Conf. IEEE Computer and Comm. Societies (INFOCOM)*, vol. 3, pp. 1587-1596, 2002.

[6] Q. Wang and W. Yang, "Energy Consumption Model for Power Management in Wireless Sensor Networks," *Proc. 4th Ann. IEEE Comm. Society Conf. Sensor, Mesh and Ad Hoc Comm. Networks (SECON'07)*, pp. 142-151, 2007.

[7] A. Konstantinidis, K. Yang, and Q. Zhang, "An Evolutionary Algorithm to A Multi-Objective Deployment and Power Assignment Problem in Wireless Sensor Networks," *Proc. IEEE Global Telecomm. Conf. (GLOBECOM)*, pp. 1-6, 2008.

[8] R. Moraes, C. Ribeiro, and C. Duhamel, "Optimal Solutions for Fault-Tolerant Topology Control in Wireless Ad Hoc Networks," *IEEE Trans. Wireless Comm.*, vol. 8, pp. 5970-5981, Dec. 2009.

[9] G. Kalpana and T. Bhuvaneswari, "Distributed Power Control for Energy Efficiency in Wireless Sensor Network," *European J. Scientific Research*, vol. 48, pp. 273-280, 2010.

[10] V. Kawadia and P.R. Kumar, "Principles and Protocols for Power Control in Ad Hoc Networks," *IEEE J. Selected Areas in Comm.*, vol. 23, pp. 76-88, Jan. 2005.

[11] M. Kubisch, H. Karl, A. Wolisz, L. Zhong, and J. Rabaey, "Distributed Algorithms for Transmission Power Control in Wireless Sensor Networks," *Proc. IEEE Wireless Comm. Networking (WCNC)*, vol. 1, pp. 558-563, 2003.

[12] I. Khemapech, A. Miller, and I. Duncan, "A Survey of Transmission Power Control in Wireless Sensor Networks," *Proc. PGNet*, pp. 15-20, 2007.

[13] S. Lin, J. Zhang, G. Zhou, L. Gu, T. He, and J.A. Stankovic, "ATPC: Adaptive Transmission Power Control for Wireless Sensor Networks," *Proc. SenSys*, pp. 223-236, 2006.
[14] L. Wolsey, *Integer Programming*. Wiley Interscience Publication, 1998.
[15] W. Heinzelman, A. Chandrakasan, and H. Balakrishnan, "An Application Specific Protocol Architecture for Wireless Microsensor Networks," *IEEE Trans. Wireless Comm.*, vol. 1, pp. 660-670, Oct. 2002.
[16] M. Rahimi, R. Baer, O. Iroezi, J. Garcia, J. Warrior, D. Estrin, and M. Srivastava, "Cyclops: In Situ Image Sensing and Interpretation in Wireless Sensor Networks," *Proc. SenSys*, pp. 192-204, 2005.
[17] M. Cheng, X. Gong, and L. Cai, "Joint Routing and Link Rate Allocation Under Bandwidth and Energy Constraints in Sensor Networks," *IEEE Trans. Wireless Comm.*, vol. 8, pp. 3770-3779, July 2009.
[18] K. Bicakci, H. Gultekin, and B. Tavli, "The Impact of One-Time Energy Costs on Network Lifetime in Wireless Sensor Networks," *IEEE Comm. Letters*, vol. 13, pp. 905-907, Dec. 2009.
[19] A. Brooke, D. Kendrick, A. Meeraus, and R. Raman, *GAMS: A User Guide*. Scientific Press, 1998.
[20] J.-R. Jiang, C.-M. Lin, and Y.-J. Hsu, "Localization with Rotatable Directional Antennas for Wireless Sensor Networks," *Proc. 39th Int'l Conf. Parallel Processing Workshops (ICPPW)*, pp. 542-548, 2010.
[21] P.K. Sahoo and I.-S. Hwang, "Collaborative Localization Algorithms for Wireless Sensor Networks with Reduced Localization Error," *Sensors*, vol. 11, pp. 9989-10009, 2011.
[22] B. Kusy, A. Ledeczi, M. Maroti, and L. Meertens, "Node Density Independent Localization," *Proc. 5th Int'l Conf. Information Processing in Sensor Networks (IPSN)*, pp. 441-448, 2006.
[23] M. Zuniga and B. Krishnamachari, "Analyzing the Transitional Region in Low Power Wireless Links," *Proc. 1st Ann. IEEE Comm. Society Conf. Sensor and Ad Hoc Comm. Networks (IEEE SECON)*, pp. 517-526, 2004.
[24] J. Vales-Alonso, E. Egea-Lopez, A. Martinez-Sala, P. Pavon-Marino, M.V. Bueno-Delgado, and J. Garcia-Haro, "Performance Evaluation of MAC Transmission Power Control in Wireless Sensor Networks," *Computer Networks*, vol. 51, pp. 1483-1498, 2007.
[25] M. Mallinson, P. Drane, and S. Hussain, "Discrete Radio Power Level Consumption Model in Wireless Sensor Networks," *Proc. IEEE Int'l Conf. Mobile Adhoc and Sensor Systems (MASS)*, pp. 1-6, 2007.
[26] G. Hackmann, O. Chipara, and C. Lu, "Robust Topology Control for Indoor Wireless Sensor Networks," *Proc. SenSys*, pp. 57-70, 2008.
[27] S.K. Mitra, J. Banerjee, P. Ghosh, and M.K. Naskar, "Analysis of Network Lifetime for Wireless Sensor Network," *Int'l J. Computer Applications*, vol. 32, pp. 39-45, 2011.
[28] N. Aslam, W. Robertson, and W. Phillips, "Clustering with Discrete Power Control in Wireless Sensor Networks," *Proc. 3rd Int'l Conf. Sensor Technologies and Applications (SENSORCOMM)*, pp. 43-48, 2009.
[29] N. Aslam, W. Robertson, and W. Phillips, "Performance Analysis of WSN Clustering Algorithms Using Discrete Power Control," *IPSI Trans. Internet Research*, vol. 5, pp. 10-15, 2009.
[30] F. Sun and M. Shayman, "Lifetime Maximizing Adaptive Traffic Distribution and Power Control in Wireless Sensor Networks," ECE Dept., Univ. of Maryland, Technical Report TR2006-12, 2006.

Huseyin Cotuk received the BSc degree (valedictorian) in electronics and communications engineering from Suleyman Demirel University, Isparta, Turkey in 2002. He received the MSc degree in computer engineering from TOBB-ETU, Ankara, Turkey in 2008. He is pursuing the PhD degree in computer engineering at TOBB-ETU. He is currently a senior network engineer at TUBITAK ULAKBIM, Ankara, Turkey. His current research areas include networking and optimization.

Kemal Bicakci has obtained the PhD degree from Middle East Technical University, Ankara, Turkey in 2003. He is currently an associate professor in the Computer Engineering Department, TOBB-ETU, Ankara, Turkey. His research interests include wireless and sensor networks, information security, applied cryptography, and usability.

Bulent Tavli received the BSc degree in electrical and electronics engineering from the Middle East Technical University, Ankara, Turkey in 1996. He received the MSc and PhD degrees in electrical and computer engineering from the University of Rochester, Rochester, New York, in 2001 and 2005, respectively. He is currently an associate professor in the Electrical and Electronics Engineering Department, TOBB-ETU, Ankara, Turkey. His current research areas include telecommunications and embedded systems.

Erkam Uzun received the BSc degrees in both computer engineering and electrical and electronics engineering from TOBB-ETU, Ankara, Turkey in 2011. He is currently an MSc student with the Computer Engineering Department, TOBB-ETU, Ankara, Turkey. His current research areas include telecommunications, digital forensics, multimedia computing, and security.

▷ **For more information on this or any other computing topic, please visit our Digital Library at** www.computer.org/publications/dlib.